

CHARACTERIZATION AND OPTICAL PROPERTIES OF CdSe NANO-CRYSTALLINE THIN FILMS

R. S. SINGH^{*}, S. BHUSHAN^a, A. K. SINGH^b, S. R. DEO^b

Deptt. of Physics, Govt. D. T. College Utai, Durg-491107 (C. G.), India

^aShri Shankaracharya Engineering College Bhilai, Durg-490020 (C.G.), India

^bDeptt. of Chemistry, Govt. VYT PG College Durg-491001 (C.G.), India

Chemical bath deposition (CBD) was used to prepare a CdSe semiconductor films on glass substrates. Scanning electron microscopic studies shows ball type structures with approximate grain size ranging between 4 nm and 8 nm with voids on uniform background. The crystallographic structure of the film and the size of the crystallites in the film were studied by X-ray diffraction. XRD measurement shows that the film is crystallized in the wurtzite phase and presents a preferential orientation along the c-axis. Optical constants such as refractive index n and extinction coefficient k , were determined from transmittance spectrum in the ultraviolet-visible (UV-VIS) regions using envelope methods. Absorption coefficient α and the thickness of the film t were calculated from interference of transmittance spectra. Optical excitation spectra showed maximum excitation at 389 nm. The photoluminescence (PL) emission spectra under this excitation consisted of two peaks at 485 nm and 531 nm wavelengths, which are attributed to the presence of one deep trapping site and electron hole recombination via trap state or imperfection site. The blue shift observed in the PL emission spectra corresponds to the nano-crystalline effect.

(Received September 30, 2010; accepted January 31, 2011)

Keywords: Chemical bath deposition, Energy band-gap, X-ray diffraction, Photoluminescence.

1. Introduction

The II-VI binary semiconducting compounds, belonging to the cadmium chalcogenide family (CdS, CdSe, CdTe) are considered to be very important due to their potential use in photoconductive devices and solar cells [1-4]. Cadmium selenide thin film has widely been studied because of its high absorption coefficient and nearly optimum band gap energy (1.73 eV), and it finds a wide range of applications in low cost devices such as light emitting diodes, solar cells, photodetectors, electro photography and laser [1,4-6]. The methods commonly used for depositing CdSe thin films are chemical bath deposition (CBD) [1,5,6], vacuum evaporation [7], electro-deposition [8], spray pyrolysis [9], thermal evaporation [10], successive ionic layer adsorption and reaction (SILAR) [11]. CBD has many advantages as compared to other technologies, in particular the low fabrication cost and the growth repeatability. The process is readily scalable to large-area processing [12].

In this work, CdSe thin films were deposited by CBD technique on glass substrates and their morphological, structural and optical properties are presented and discussed. The widely used envelope method [13] has been developed for optical transmittance measurements to evaluate the thickness (t), absorption coefficient (α), extinction coefficient (k), which is defined as the imaginary part of the complex refractive index.

*Corresponding author: rss.bhilai@gmail.com

2. Experimental details

Substrates used in the present work were commercial quality microscopic glass slides of dimensions 24mm x75mm, which were first cleaned with HCl, acetone, distilled water and ultrasonic cleaner. They were then dried and dipped vertically into a mixture of solutions of 1M cadmium acetate, triethanolamine (TEA), sodium selenosulphate (prepared by heating sodium sulphite with selenium at 90°C for 5 hrs.) and 30% aqueous ammonia. All solutions were prepared in double distilled water. TEA was used as a complexing agent to form $\text{Cd}[\text{TEA}]^{2+}$ complex for controlling the growth rate. thiophenol and methanol (in 1:1 ratio) was used as the capping agent [13] to the above said mixture of solutions, for preparing the nano-crystalline films. The films were then formed on glass substrates by dipping them vertically in the solution, kept in a constant temperature water bath at 60°C for 60 minutes. The deposition of films is based on precipitation followed by condensation. After deposition, the films were washed with double distilled water and then dried at room temperature.

The structural properties were studied by X-ray diffraction measurements using RIGAKU X-Ray Diffractometer with $\text{CuK}\alpha$ ($\lambda = 1.54056 \text{ \AA}$) radiation. The average dimension of crystallites was determined by the Scherrer method [16] from the broadening of the diffraction peaks taking into account the instrumental broadening.

The morphological features of the CdSe thin films were studied by JEOL JSM-5600 scanning electron microscope and the optical measurements of the crystalline CdSe thin film were carried out at room temperature using Shimadzu UV-VIS 1700 scanning spectrophotometer in the wavelength range from 350 to 800 nm. Swanepoel's envelope method was employed to evaluate the optical constants such as the refractive index n , extinction coefficient k and absorption coefficient α from transmission spectra [14]. The thickness of the crystalline CdSe thin film was determined from interference fringes of transmission data measured over the visible range. The optical excitation and PL emission spectra were studied by using Shimadzu flurospectrophotometer (RF 5301) under 389 nm excitation.

3. Results and discussion

3.1 SEM Studies

Scanning electron microscopy (SEM) is a convenient technique to study microstructure of thin films. Figs. 1(a) and (b) show the SEM pictures of the CdSe films of sample A and B respectively. Role of capping agents is to avoid coalescenceness of particles and thus particle size reduces. As the concentration of capping agent increases, particle size is expected to reduce further because of the more avoidance of coalescenceness of different particles in presence of capping agents and this obviously can be seen from the micrographs. Almost spherical ball type structures with approximate particle size ~8 nm in sample A and ~4 nm in sample B, on uniform background, are observed. Particle size and voids are found to decrease with increase in volume of capping agent.

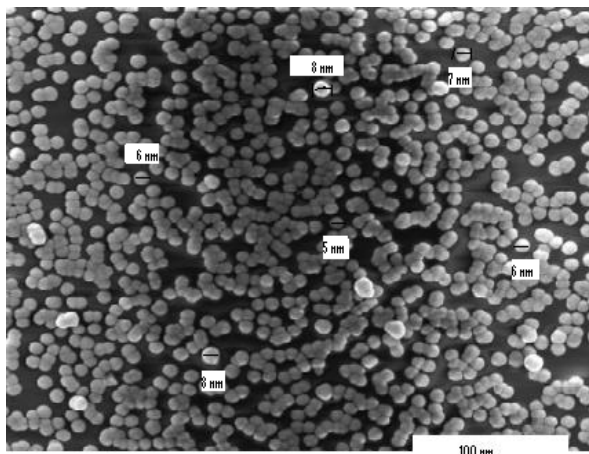


Fig 1(a) SEM Micrograph of CdSe thin film using 0.2 ml of capping agent

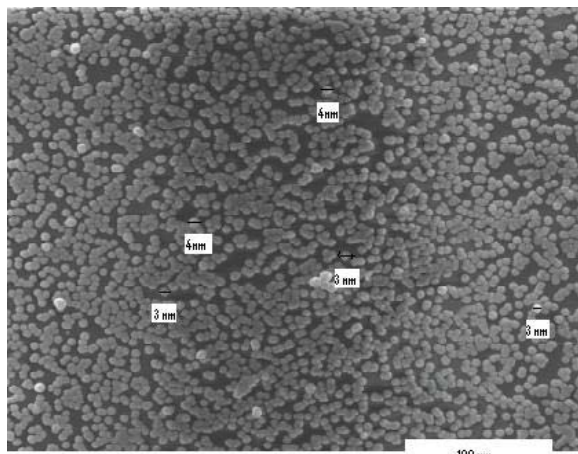


Fig 1(b) SEM Micrograph of CdSe thin film using 0.5 ml of capping agent

3.2 Structural properties of the crystalline CdSe thin film

The crystal structure and orientation of the CdSe thin films were investigated by X-ray diffraction (XRD) patterns. The X-ray diffraction spectra for the crystalline CdSe thin film shown in fig. 2, indicate that the film is of polycrystalline nature. Data analysis revealed the formation of nano-crystalline CdSe with wurtzite (hexagonal) structure. For both samples, the peak at lower angles is the envelope of several reflections; therefore, this region cannot be used to evaluate the domain dimensions. However, the large full-width-at-half-maximum of the peaks at the highest angles gives a clear indication of the nanometer domain size [15].

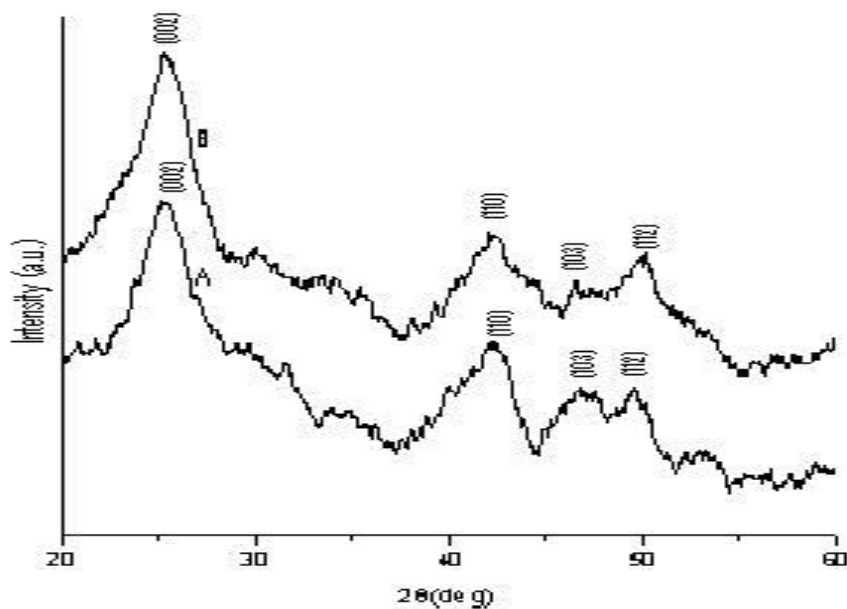


Fig -2 XRD diffractogram of different samples : (A) CdSe thin film using 0.2 ml capping agent, (B) CdSe thin film using 0.5 ml capping agent.

The grain size of crystallites was calculated using a well-known Scherrer's formula [16] :

$$D = \frac{0.9\lambda}{\beta \cos\theta} \quad (1)$$

where D is the grain size of crystallite, λ the wavelength of X-rays used, β the broadening of diffraction line measured at half its maximum intensity in radians and θ is the angle of diffraction. The value found for the average grain size corresponding to the (002) peak for sample A is 6.92 nm and for sample B is 3.67 nm. This decrease in grain size with increase in volume of capping agent supports the nano- crystalline effect.

The texture coefficient (TC) represents the texture of the particular plane, deviation of which from unity implies the preferred growth. Quantitative information concerning the preferential crystallite orientation was obtained from the different texture coefficient $TC(hkl)$ defined as [17]

$$TC(hkl) = \frac{I(hkl)/I_0(hkl)}{N^{-1}\sum I(hkl)/I_0(hkl)} \quad (2)$$

n

where $I(hkl)$ is the measured relative intensity of a plane (hkl) , $I_0(hkl)$ is the standard intensity of the plane (hkl) taken from the JCPDS data [18], N is the reflection number and n is the number of diffraction peaks. A sample with randomly oriented crystallite presents $TC(hkl)=1$, while the larger this value, the larger abundance of crystallites oriented at (hkl) direction. The calculated texture coefficients are presented in Table 1. It can be seen that the highest TC was in (002) plane for CdSe thin film.

Table 1
The texture coefficients of CdSe

Systems	2θ (deg)	(hkl)	d(Å)	I/I ₀	TC(hkl)
Sample A	25.354	(002)	3.5099	100	3.956
	41.968	(110)	2.1509	0.291	0.012
	45.788	(103)	1.98	0.323	0.013
	49.669	(112)	1.834	0.494	0.02
Sample B	25.344	(002)	3.5094	100	3.953
	41.896	(110)	2.1508	0.36	0.014
	45.781	(103)	1.96	0.3	0.012
	49.662	(112)	1.832	0.53	0.021

3.3 Optical properties of the crystalline CdSe thin film

Fig. 3 shows transmittance and reflectance curves for the crystalline CdSe thin film, where the film due to interference phenomena between the wave fronts generated at the two interfaces (air and substrate) defines the sinusoidal behavior of the curves' transmittance vs. wavelength of light. CdSe thin film showed interference fringe pattern in transmission spectrum in the infra-red (IR) region. This revealed the smooth reflecting surfaces of the film and there was not much scattering loss at the surface. A metal rich film usually exhibits less transparency. High transmittance > 80% in the visible region has been observed which may be used in applications in solar cells.

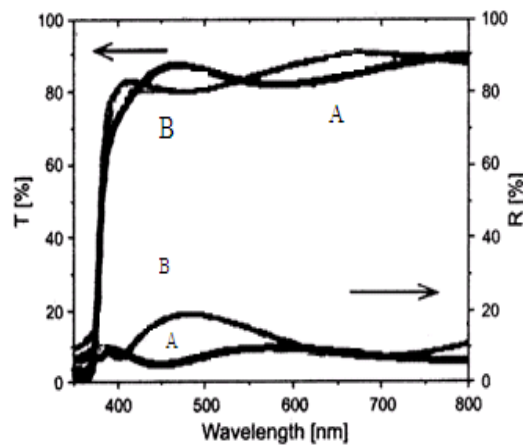


Fig. 3 Optical transmission and reflection spectra of different samples : (A) CdSe thin film using 0.2 ml capping agent, (B) CdSe thin film using 0.5 ml capping agent.

The excellent surface quality and homogeneity of the film were confirmed from the appearance of interference fringes in the transmission spectra. This occurs when the film surface is reflecting without much scattering/absorption in the bulk of the film. The films exhibited good transparency in the visible region.

The refractive index is an important parameter for optical materials and applications. Thus, it is important to determine optical constants of the films and the complex optical refractive indices of the films are described by the following relation [19] :

$$n' = n(\omega) + ik(\omega) \quad (3)$$

where n is the real part and k is the imaginary part (extinction coefficient) of complex refractive index. The refractive index n at different wavelengths was calculated using the envelope curve for T_{\max} (T_M) and T_{\min} (T_m) in the transmission spectra [14]. The expression for refractive index is given by

$$n = [N + (N^2 - n_s^2)^{0.5}]^{0.5} \quad (4)$$

where

$$N = 2n_s \frac{T_M - T_m}{T_M T_m} + \frac{N_s^2 + 1}{2} \quad (5)$$

and n_s is the refractive index of the substrate [in our case $n_s = 1.52$ (glass)].

The extinction coefficient k can be obtained from the experimental expression [20]:

$$k = \frac{\alpha \lambda}{4\pi d} \quad (6)$$

$$\alpha = -\frac{1}{t} \ln \frac{(n-1)(n-n_s)((T_{\max}/T_{\min})+1)^{0.5}}{(n+1)(n+n_s)((T_{\max}/T_{\min})-1)^{0.5}} \quad (7)$$

where α is the absorption coefficient and t is the film thickness. The optical constants such as refractive index n and extinction coefficient k were determined from a transmittance spectrum in the wavelength range 350-800 nm by envelope method. The variations of refractive index n and extinction coefficient k with wavelength λ in this region are shown in figs 4 and 5, respectively. Although extinction coefficient values increase with increasing wavelength, the refractive index values decrease.

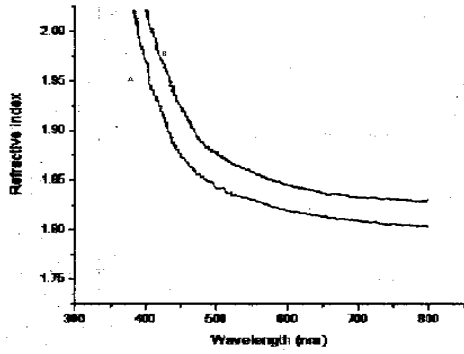


Fig. 4 Plot of refractive index as a function of wavelength of different samples : (A) CdSe sample using 0.2 ml capping agent, (B) CdSe using 0.5 ml capping agent.

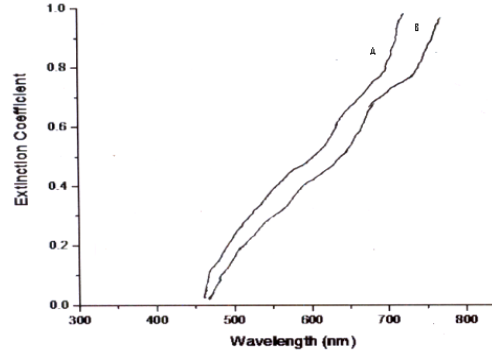


Fig. 5 Plot of extinction coefficient as a function of wavelength of different samples : (A) CdSe sample using 0.2 ml capping agent, (B) CdSe using 0.5 ml capping agent.

The thicknesses of the films has been calculated using the equation :

$$t = \frac{\lambda_1 \lambda_2}{2(\lambda_1 n_2 - \lambda_2 n_1)} \quad (8)$$

where n_1 and n_2 are the refractive indices corresponding to wavelengths λ_1 and λ_2 , respectively [14]. The thicknesses of the two films were found to be 0.635 μm and 0.648 nm respectively.

The absorption coefficient α of the CdSe film was determined from transmittance measurements. Since envelope method is not valid in the strong absorption region, the calculation of the absorption coefficient of the film in this region was calculated using the following expression:

$$\alpha(\nu) = 2.303(A/t) \quad (9)$$

where A is the optical absorbance.

Plot of the function $\alpha = f(h\nu)$, shown in fig. 6 could be subdivided into two regions [21]. The first region is for higher values of absorption coefficient, namely for $\alpha(h\nu) > 10^4 \text{ cm}^{-1}$, this corresponds to transitions among extended states in both valence and conduction bands, where the power law of Tauc [22] :

$$\alpha h\nu = B(h\nu - E_g)^{0.5} \quad (10)$$

is valid for direct transitions. The variation of $(\alpha h\nu)^2$ with photon energy $h\nu$ for the CdSe thin film is shown in Fig. 7. It has been observed that the plots of $(\alpha h\nu)^2$ versus $h\nu$ are linear over a wide range of photon energies indicating the direct type of transitions. The intercepts (extrapolations) of these plots (straight lines) on the energy axis give the energy band gaps. From this drawing, the

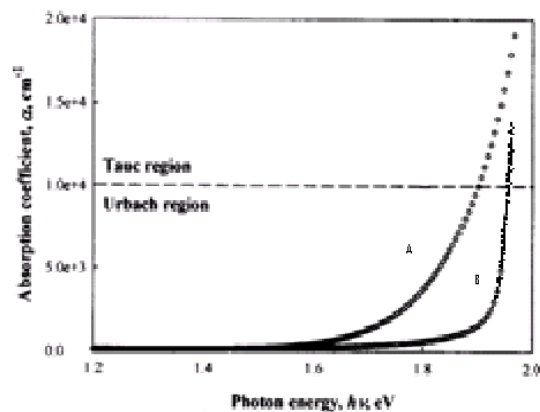


Fig. 6 Absorption coefficient as a function of photon energy for different samples : (A) CdSe thin film using 0.2 ml capping agent, (B) CdSe thin film using 0.5 ml capping agent. The dashed line differentiates the Tauc and Urbach regions.

band gap, $E_g = 1.77$ eV and 1.89 eV for sample A and B, respectively, is obtained.

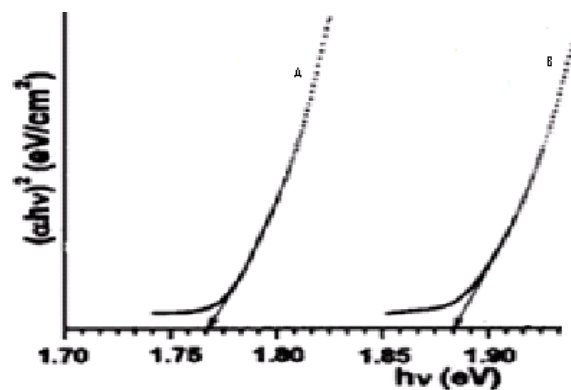


Fig. 7 Tauc's plot for determining optical energy gap of indirect transitions for different samples : (A) CdSe thin film using 0.2 ml capping agent, (B) CdSe thin film using 0.5 ml capping agent.

The second region for $\alpha = f(h\nu)$ is for lower value of α that is for $\alpha = f(h\nu) < 10^4 \text{ cm}^{-1}$, where the absorption coefficient presents a roughly exponential behavior :

$$\alpha = \alpha_0 \exp (h\nu/E_u) \quad (11)$$

where α_0 is a constant and E_u is Urbach energy interpreted as the width of the tails of localized states, associated with the amorphous state, in the forbidden gap. The absorption in this region is due to transitions between the extended states in one of the bands and localized states in the exponential tail of the other band [23,24]. The inverse slope or the width of the exponential edge (E_u) reflects the width of the more extended band tail that is often called Urbach energy. Such exponential or Urbach edge is usually ascribed to localized states at the band edges. In other words, the Urbach edge is determined by the degree of disorder (e.g. charged impurities) and /or structural defects (e.g. broken or dangling bonds, vacancies, non-bridging atoms or chain ends) in the considered semiconductor material [25]. The structural defects are collected together or assembled with impurities thus forming defect complexes in order to obtain a lower energy state. The $\ln(\alpha)$ vs. photon energy plots for the CdSe thin film is shown in fig. 8. The value of E_u obtained from this figure is 71.88 meV.

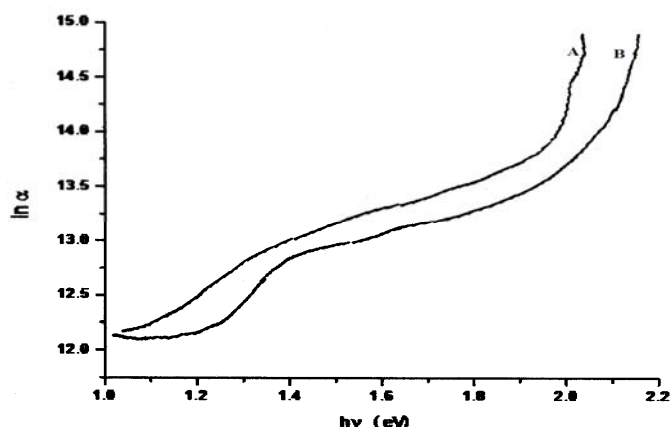


Fig. 8 Urbach plot of different samples: (A) CdSe thin film using 0.2 ml capping agent, (B) CdSe thin film using 0.5 ml capping agent.

The particle sizes are calculated using the formula [26]

$$E_{gn} = [E_{gb}^2 + 2\hbar^2 E_{gb}(\pi/R^2)/m^*]^{1/2} \quad (26)$$

where E_{gn} & E_{gb} are the band gap of nano-crystallites, and bulk semiconductor (1.73 eV) respectively, R is the particle radius and m^* is the effective mass of electron. Substituting the values of E_{gn} determined above (1.77 eV and 1.89 eV for samples A and B respectively) and standard values of other parameters, the particle sizes of samples A and B were found to be 6.7583 nm and 3.3227 nm respectively. These values are very close to the values obtained from the SEM and XRD studies.

3.4 PL excitation and emission studies of the crystalline CdSe thin film

The optical excitation and PL emission spectra under 389 nm excitation of CdSe thin film, which were recorded at room temperature, are shown in fig. 9. It is observed that with increase in volume of capping agent, the intensity of PL emission peaks improves. Sample B has slightly lower grain size whose PL spectrum shows an intense band in the green region (531 nm) and a less intense in the blue region (485 nm). This is associated with decrease of particle size with increase in volume of capping agent. The band gap of the CdSe film in sample B is about 1.89 eV and the emission band values observed in PL studies are very much blue shifted. Such a large Stokes shift between the optical absorption spectrum and PL emission band may be attributed to the presence of one deep trapping site and electron hole recombination via trap state or imperfection site (donor here) [27]. Such lattice phenomena are observed in nano materials and these results confirm the nano-crystalline nature of the chemically deposited CdSe film in the present study. Deep states in nano-crystalline materials are mainly associated with stoichiometric defects, dangling bonds or external atoms such as oxygen [28].

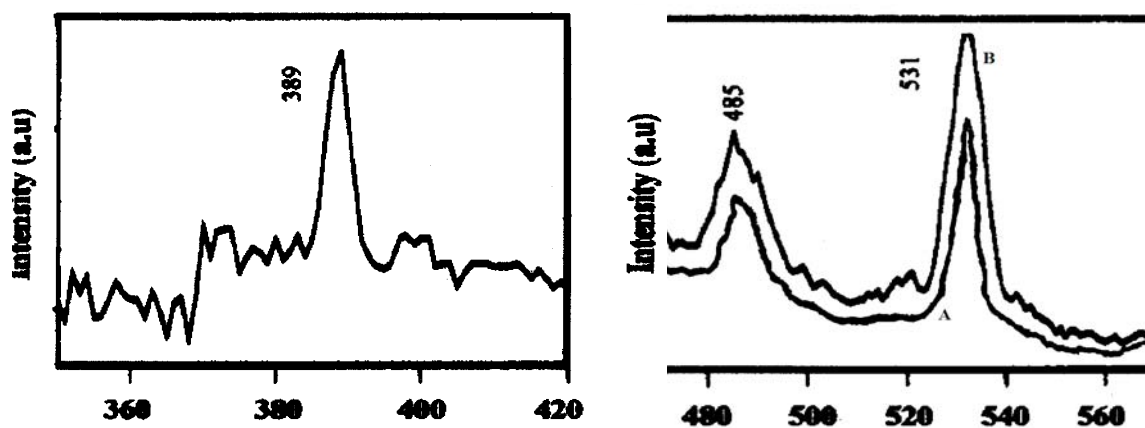


Fig. 9(a) Optical excitation spectrum of CdSe thin film.

Fig. 9(b) PL emission spectra of different sample : (A) CdSe thin film using 0.2 ml capping agent, (B) CdSe thin film using 0.5 ml capping agent.

4. Conclusions

CdSe nano-crystalline thin films have been deposited onto glass substrates by the chemical bath deposition method at 60^o C temperatures. Ball type structures (spherical grains of approximate size ranging between 4 nm and 8 nm) with voids on uniform background are seen in the SEM micrographs. The X-ray diffraction patterns of the crystalline CdSe thin films reveal the existence of a CdSe single-phase with a hexagonal wurtzite structure. The XRD patterns consist of (002) main peak, which is due to CdSe crystals that grow along the c-axis. Optical constants such as refractive index n and extinction coefficient k were determined from transmittance spectrum in the UV-VIS regions using envelope method. The thickness of the film t was calculated from interference of transmittance spectra. Also, energy band gap values (E_g) and Urbach energy (E_u) were calculated. In conclusion, the deposited crystalline CdSe thin film was suitable for many optical devices, such as solar cells, because of well-crystallized, high transmittance in visible region (> 80%) and suitably wide band gap value. PL emission spectra (under 389 nm excitation) exhibits blue shift (nano-crystalline effect), consisting of two peaks at 485 nm and 531 nm wavelengths.

Acknowledgement

The authors gratefully acknowledge UGC-CRO, Bhopal for providing the financial assistance through the project F.N.-MS-56/202024/09-10 to one of the authors (RSS).

References

- [1] P. P. Hankare, V. M. Bhuse, K. M. Garadkar, S. D. Delekar, and I. S. Mulla, *Semicond. Sci. Technol.* **19**, 70 (2004).
- [2] K. R. Murali, V. Swaminathan, and D. C. Trivedi, *Sol. Energy Mater. Sol. Cells* **81**, 113 (2004).
- [3] J. Y. Choi, K. J. Kim, J. B. Yoo, and D. Kim, *Sol. Energy* **64**, 41 (1998).
- [4] P. O'Brien and J. McAleese, *J. Mater. Chem.* **8**, 2309 (1998).
- [5] S. Gorer and G. Hodes, *J. Phys. Chem.* **98**, 5338 (1994).
- [6] M. T. S. Nair, P. K. Nair, R. Zingaro, and E. A. Moyers, *J. Appl. Phys.* **74**, 1879 (1993).
- [7] K. Subba Ramaiah, Y. K. Su, S. J. Chang, F. S. Juang, K. Ohdaira, Y. Shiraki, H. P. Liu, I. J. Chen, and A. K. Bhatnagar, *J. Cryst. Growth* **224**, 74 (2001).
- [8] S. M. Rashwan, S. M. Abdul-Wahab, and M. M. Mohammed, *J. Mater. Sci. Mater. Electron.* **18**, 575 (2007).

- [9] Yu. V. Melelera, N. A. Redy Chev, and G. F. Nevikor, *Inorg. Mater.* **43**, 455 (2007).
- [10] K. N. Shreekanthan, B. V. Rajendra, V. B. Kasturi, and G. K. Shivakumar, *Cryst. Res. Technol.* **38**, 31 (2003).
- [11] O. Yomamoto, T. Sasamoto, and M. Inagaki, *J. Mater. Res.* **13**, 3394 (1998).
- [12] C. Vargas-Hernández, V. C. Lara, J. E. Vallejo, J. F. Jurado, and O. Giraldo, *phys. stat. sol. (b)* **242**, No. 9, pp. 1897–1901 (2005).
- [13] S. Bhushan and S. Shrivastava, *Cryst. Res. Technol.* **42**, 10 (2007).
- [14] R. Swanepoel, *J. Phys. E: Sci. Instrum.* **16**, 1214 (1983).
- [15] Mauro Epifani, Cinzia Giannini, Liberato Manna: *Materials Letters* **58**, pp. 2429– 2432 (2004).
- [16] B. D. Cullity, S. R. Stock, *Elements of X-Ray Diffraction*, 3rd ed. Prentice Hall, 2001.
- [17] C. S. Barret, T. B. Massalski, *Structure of Metals*, Pergamon Press, Oxford, 1980.
- [18] Joint Committee on Powder Diffraction Standards, *Powder Diffraction File*, card no: 8-0459.
- [19] Yakuphanoglu F., Cukurovali A., Yilmaz I., *Optical Materials* **27**(8), pp. 1363–1368 (2005).
- [20] J. C. Manificier, J. Gasiot, J. P. Fillard, *J. Phys. E* **9**, 1002 (1976).
- [21] J. Tauc, *Amorphous and Liquid Semiconductors*, Plenum, New York, 1974; *ibid*, *Phys. Status Solidi* **15**, 62 (1996).
- [22] N. F. Mott, R. W. Gurney, *Electronic Processes in Ionic Crystals*, Oxford Univ. Press, London, 1940.
- [23] M.H. Cohen, C.M. Soukoulis, E.N. Economou, *AIP. Conf. Proc.* **120** (1984).
- [24] F. Urbach, *Phys Rev.* **92**, 1324 (1953).
- [25] N.F. Mott, E.A. Davis, *Electronic Processes in Non-Crystalline Materials*, Clarendon Press, Oxford, 1979.
- [26] Y. Wang and N. J. Herron, *Phys. Chem.* **91**, 257 (1987).
- [27] S. Chaure, N. B. Chaure, and R. K. Pandey, *Physica E* **28**, 439 (2005).
- [28] A. S. Edeleestein and R. C. Camarata, *Nanomaterials: Synthesis, Properties and Application* (Institute of Physics Publishing, 1998), p. 214, 230, 235, 241.